Lasers in Manufacturing Conference 2015

On Line Evaluation of Femtosecond Laser Ablation Efficiency on Copper Structures

J. S. Hoppius, A. Kanitz, E. L. Gurevich, A. Ostendorf

[a]*Applied Laser Technologies, Ruhr-University Bochum, Universitätsstr.150, 44801 Bochum, Germany*

Abstract

Femtosecond laser ablation is a flexible method to generate precise structures in the micrometer range. Yet, the efficiency for the removal of bulk material is lower than ablation with micro- or nanosecond pulses. To evaluate the efficiency of ultrashort pulse material ablation copper, test stripes were prepared and partly ablated with a titanium sapphire laser. The electrical resistance of material is inversely proportional to its wire cross-section. Therefore, the change of resistance is an indirect measure for the removed material. This instantaneous feedback enables on line optimization of laser processing parameters. The results for various repetition rates, spot overlaps, ablation strategies and pulse energies with pulse durations of 35 femtoseconds are compared with surface profiles measured by white-light interferometry.

Keywords: femtosecond laser ablation; copper; electrical resistance; in situ evaluation

1. Introduction

Ultra short pulse laser ablation convinces due to its nearly perfect manufacturing results. Well defined structure processing in the lower micrometer range is stable and reproducible since random material melting and sprinkle processes are negligible [Chichkov et al]. Ultrashort pulse laser manufacturing arrives in industry nowadays not only in high precision micro- and nano-fabrication but also in conventional continuous wave and long pulse applications. Major reasons for this trend are better results due to smaller heat affected zones which reduces additional costs for post processing and market maturity of industrial one-box ultrashort pulse (USP) laser systems with acceptable price levels. Nevertheless the various

interaction mechanisms of light and matter are not totally understood and especially for heterogeneous materials or complex structures barely predictable.
Therefore, identification of all process requirements and determination of optimal processing parameters is one of the most challenging tasks to ensure a stable and yet efficient USP process.
Desirable is a control and feedback system to adapt the process parameters to current manufacturing conditions. State of the art technologies are optical on-axis measurement systems like triangulation, optical coherence tomography and low coherence interferometry [Schmitt et. al] that acquire the 3D working profile on line and enable readjustments. Nevertheless the implementation of these systems in commercial laser ablation systems is neither easy to utilize nor inexpensive.

As a consequence the processing parameters are often found by parameter tests and ex situ examination with a microscope, interferometer or scanning electron microscope afterwards. However, most laser workstations possess a wide range of parameters from pulse energy, pulse shape, repetition rate, focal spot diameter, to pulse overlap distance wherefore an optimization to highest efficiency can be highly time-consuming. In this work we present an approach to accelerate parametric studies for ultrashort pulse ablation based on conducting materials.

2. Measurement Principle and Experimental Setup

Every laser spot induces a defined amount of photon energy and ablates a material volume dependent on light absorption, material threshold and pulse and material shape. For a focused beam on a flat surface a theoretical model to describe the sublimation volume was presented by Neuenschwander et al..

Figure 1a shows the intensity distribution of a Gaussian beam focused onto a flat surface whereas the above ablation threshold energy is indicated in green. This part of the beam has sufficient intensity to sublimate material at the surface while the red areas do not exceed the threshold. For higher pulse energies the cold ablation area increases accordingly.

Furthermore, the sublimation depth is dependent on the laser beam profile which in this case is a Gaussian beam with its maximum intensity at the beam center and decreasing intensity to the edges (comparable Figure 1b). Beer-Lambert's law describes the attenuation of light in partly transparent media and can also be used to explain the attenuation during sublimation processes Neuenschwander. Therefore the ablated profile is not rectangular but parabolic like indicated for one to five pulses. The ablated volume per pulse stays nearly constant up to the material break-through whereupon only ablation at the borehole

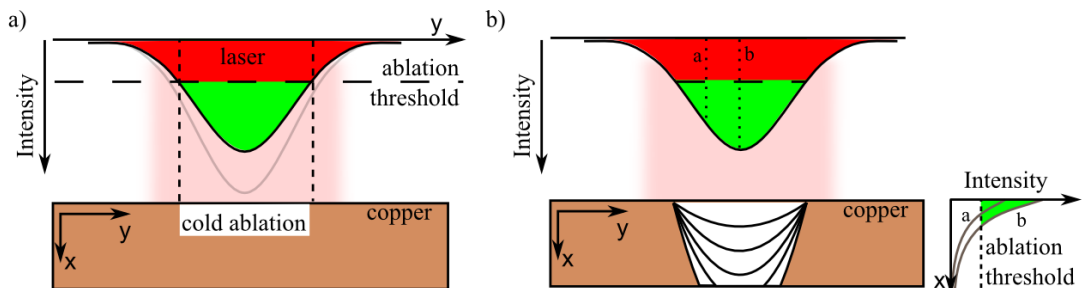

Figure 1: a) The cold ablation theory with ultrashort laser pulses is valid for pulse intensities above the material threshold (green). Nevertheless the residual pulse energy (red) is converted into heat in the material. b) For a Gaussian beam shape the cold ablated profile is parabolic. It is indicated for one to five pulses.

wall takes place. For the sake of simplicity, incubation effects are neglected.

For a conductive material stripe as target, the electrical resistance is dependent on its material specific resistivity ρ, its length l in current direction and its cross section A.

$$R = \frac{\rho \cdot l}{A} \qquad 1.1$$

After the ablation of material (comp. Figure 2a) from the surface, the total change of resistance is dependent on the shape and quantity of ablation. The total resistance is approximately the equivalent circuit of a series circuit.

$$R_{total} = \sum R_i \qquad 1.2$$

Accordingly, the total resistance is an indirect measure for the ablated volume as long as the ablation path and the basic material dimensions are known. To evaluate this correlation, a copper test structure was developed that was produced by chemical etching (comp. Figure 2b). It consists of two test pads with a displacement of 10 mm, joint by a 5µm high and 100µm broad connection.

A constant electrical current was induced by two testing pins at the outside of the structure while the resulting voltage was measured between two additional testing pins. This four-wire-sensing method avoids any disturbing contact and wire resistances of the measurement device.

The theoretical total resistance between both testing pins for the idealized rectangular copper structure and a resistivity of $1.721 \cdot 10^{-2}$ Ω·mm²/m is 354.32 mΩ. With a simplified model of rectangular cuboid shaped ablation volumes, the resistance dependent on the number of laser pulses for one ablation line straight through the joint was calculated. Since the resistance scales quadratic with the residual cross section, the change increases when/as the residual cross section gets smaller. For effective femtosecond copper ablation the incident laser fluence has to be above 0.18 J/cm² (Hashida et al.). The ablation rate of copper with a 10µm wide focal spot, 25µJ pulse energy, 35 J/cm² laser fluence respectively, and 35 fs pulse duration was determined by white light interferometry to be approximately 51,5 µm³ per pulse. For a single laser shot onto the untreated structure, the change of resistivity is in the µΩ-range. To increase the signal change of this hardly measurable effect, multiple ablation areas along the connection line are processed. The theoretical resistance variation for two hundred ablation lines parallel to each other is plotted in Figure 3. Five shots per ablation line onto the untreated structure result in a resistance change of approximately 2mΩ.

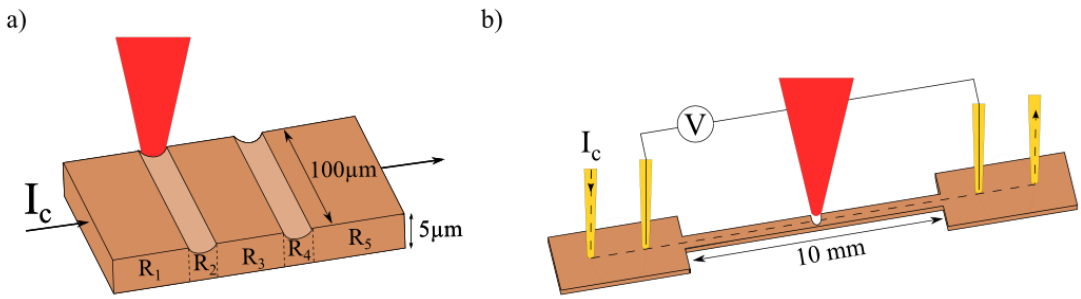

Figure 2: a) The total resistance of a copper test stripe is equal to the sum of each ressistance orthogonal to the current direction. b) The resistance determination is implemented by a four wire measurement with a constant current and a decoupled voltmeter.

With a precise current source (Keithley K2400) and a digital oscilloscope (Agilent Technology DSO1022A) resistance variations in this range are well resolvable.

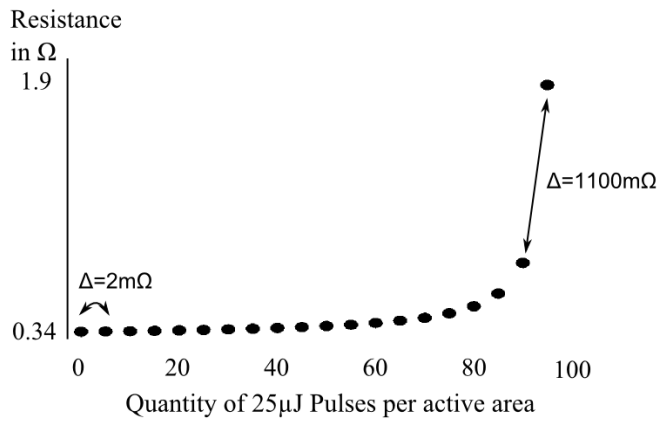

Figure 3: For given copper test stripe dimensions of 10 mm length, 5 µm height and 100 µm widths the theoretical resistance

The experimental ablation setup consisted of a titanium sapphire based chirped pulse amplification laser system (Spitfire Ace-35f) in combination with a lambda quarter plate and a polarizing prism to reduce the pulse energy. Beam guidance and focusing was implemented by a galvanometric scanner system (ScanLab7) and an 80 mm telecentric focusing lens. The experimental ablation parameters were repetition rates from single-pulse to 1 kHz double or triple pulse bursts, 8.3, 12.5 and 25.0 µJ pulse energy, 10 µm spot size and a pulse overlap length of 1, 2 and 4 µm.

3. Results

3.1. Single Pulse Experiment with 25 µJ and 4 µm Overlap

The nonlinear resistance was measured during femtosecond laser ablation with 4 µm pulse overlap (about 50%). The ablation strategy is indicated in the microscope image of an ablated structure (Figure 4b). Two hundred active ablation lines orthogonal to the current direction were ablated with one hundred 25 µJ laser shots per line. The first point was chosen to be in the material because side effects at the material borders are negligible. The ablation process never cuts the connection and the final resistance converges to a finite value accordingly. Every line was processed five times with 20 pulses and a pulse overlap of 4 µm. The processing sequence started with shot #1 (red) in active area #1, continued to ablate the first spot of every active ablation line and moved on with shot #2 (grey) in active area #1. After 20 laser shots (green) per line the process restarts at its origin four times. Therefore the measured resistance profile (comparable Figure 4a) is divided into five tracks.

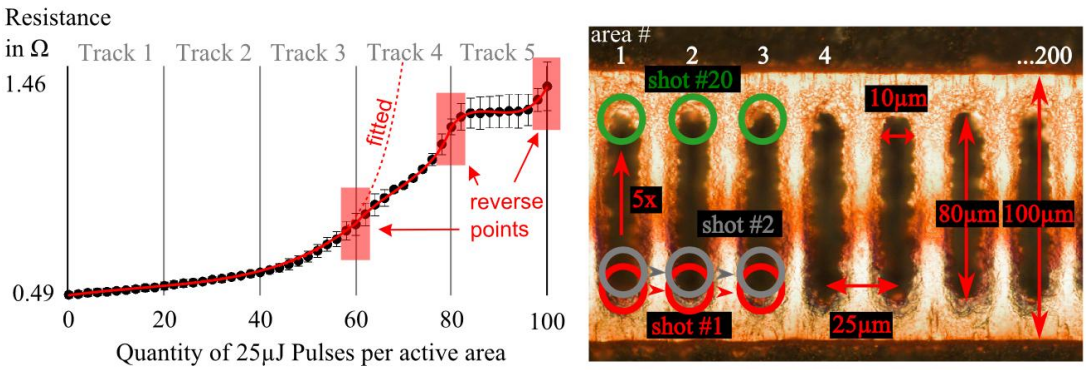

Figure 4: The resistance progress dependent on single pulse ablation for each active area has a nearly quadratic shape from one to sixty shots. After this the cutting kerf is at least partly opened and the ablation efficiency decreases strongly. Around the reverse points the resistance still changes.

It has to be mentioned, that the starting resistance of the copper structures varies by 0.15 Ω from the calculated value which results from shape differences of the test structures and heterogeneities in the material and on its surface. This deviation is nearly constant for all test structures.

Considering the theoretical resistance process and a constant material ablation for the first three tracks, it is possible to fit the ideal ablation profile (see dashed line in Figure 4a). Overall the slope of the curve rises from the start to the final value for a constant volume ablation. It can be seen that the slope in track 4 and 5 decreases to nearly zero while the resistivity change at the beginning and end of each track are still high. Comparing theses results with the microscope image (see Figure 4b) it can be seen, that the ablation process at both ends of all active areas is not finished while the ablation kerf in between is clearly opened. Those are the process reverse points.

One assumption from this trend is that some laser energy already passes through the sample in track 4 and therefore the ablation efficiency decreases. However, it is not predictable whether this drop of efficiency is due to holes at each ablation spot or an already opened kerf.

3.2. Single Pulse Experiment with 25 µJ and 2 µm overlap

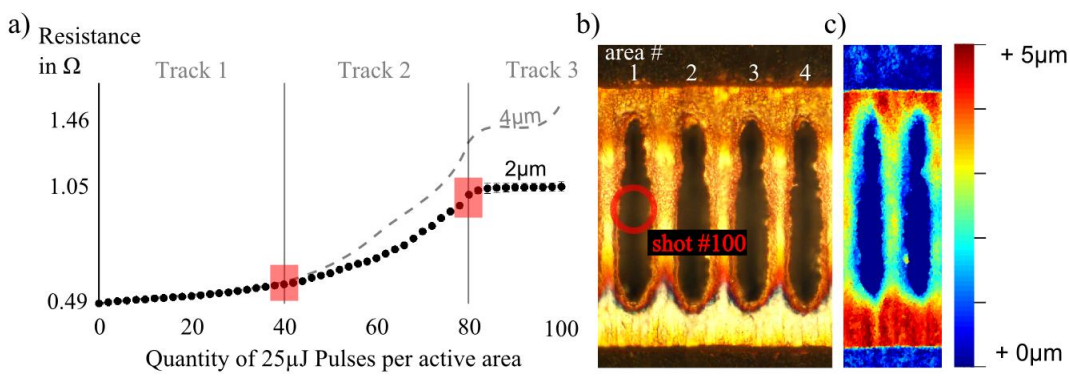

Figure 5: a) The resistance progress for 2 and 4 µm overlap is similar for 40 pulses per active area. Afterwards the efficiency goes down for the higher pulse overlap because the kerf is already opened. This can be seen in the microscopic image (b) on the upper part of each ablation line since only 2.5 tracks were processed. c) The white light interferometer image shows residual material with a thickness of up to 2 µm in this area.

With the same pulse energy and pulse duration but a different spot overlap of 2µm instead of 4µm the second experiment was realized. The measured resistance (black) is compared with the 4µm track (grey) from 3.1 (compare Figure 4). Since the spot overlap is smaller, every track consists of 40 spots to reach the same line length. The line shows a similar slope for the first 40 pulses but doesn't ascend as strong as the 4µm overlap line in track 2. After 80 spots both lines do not show any significant increase of resistance between the reverse points. Overall the total change of resistance is smaller and not as fast wherefore a lower efficiency for this ablation strategy is suspected. However, microscopic images and white light interferometry images show similar ablation profiles for 2 and 4 µm overlap (see Figure 5b). It is possible to see the different kerf profile since 100 shots only ablate two and a half tracks. In the end of each track, the kerf is thinner and residual material with a thickness up to 2 µm is not ablated. To compare the final resistance values the ablation process has to be finished with more than one hundred spots.

3.3. Pulse Burst Experiments with 25 µJ and 4 µm Overlap

Figure 6 shows the resistance progress for single, double and triple pulse burst ablation. The total applied pulse energy was 25µJ for all processes but it was divided in 2 pulses with 12.5µJ for double pulse ablation and in 3 pulses with 8.3µJ for triple pulse ablation, respectively. The repetition rate in each pulse burst is 1 kHz. The results for pulse bursts vary strongly from the single pulse processing. It can be seen that the slope for tracks one to three is higher in burst mode processing than in single pulse mode. The ablation rate between the reverse points is almost zero in track 5 for all processes but stagnates in track 4 already for double and triple pulse ablation. The fit is adapted to the triple pulse ablation rate from the beginning to the

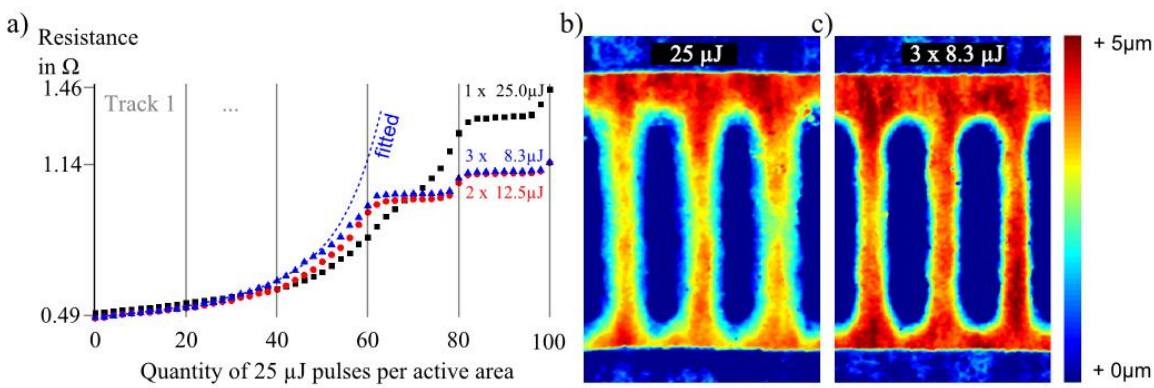

Figure 6: a) The slope of resistance change for double and triple pulse bursts is slightly higher in comparison to single pulse processing and in burst mode a saturation between the reverse points is reached earlier. b) The ablation quality is similar for two and three pulse processing but differs strongly from single pulses. The kerf is more accurate and slightly smaller.

end of track 2.

It is observed that triple pulse ablation is the most efficient regarding the beginning slope. It decreases in track three. Nevertheless the course shape is similar for double and triple pulse ablation. It has to be taken into account that the ablation kerf is smaller and more accurate for lower pulse energies due to the Gaussian pulse shape and the ablation threshold of copper [comparable 2.0]. In this experiment, the optimized parameters for this line ablation derived from the resistance measurements are triple pulse

ablation with 4µm pulse overlap. This result is in agreement with the findings of Neuenschwander et al. that the ablation is more efficient sub-1 J/cm² fluencies.

To improve the average material ablation per pulse, the ablation path could be modified. After track three, only the reverse points have to be ablated. With this adaption the necessary process energy to open the cutting kerf could be reduced by nearly 30%.

4. Outlook and Conclusion

The ablation efficiency determination by resistance measurements was proven to work with specially designed copper structures and an ultrashort pulsed laser. The first results reveal a promising method to optimize short pulse ablation strategies in order to find process parameters for conductive materials in a fast way.

For the future, it is planned to increase the pulse repetition rate to the present industry limits in the one hundred megahertz range and adapt the measurement technology. Using conductors with a lower resistivity or even semiconductors should generate higher resistance deviations per pulse and therefore enable a higher measurement accuracy and true single pulse evaluation. Further applications are the optimization of conductive layers for example for the organic solar cell production and the optimization of ablated volume rates for nano- and micro-particle production.

References

B.N. Chichkov, C. Momma, S. Nolte, F. von Alvensleben, A.Tünnermann; in Applied Physics A (Springer-Verlag, 1996), p. 109-115

R. Schmitt, G. Mallmann, K. Winands, M. Pothen; in Physics Procedia 39 (2012) p. 814-822

B. Neuenschwander, B. Jaeggi, M. Schmid, V. Rouffiange, P.-E. Martin; in SPIE LAMOM, ed. by G. Hennig, X. Xu, B. Gu, Y. Nakata (SPIE, 2012), p. 824307

M. Hashida, A.f: Semerok, O. Gobert, G. Petite, Y. Izawa, J.F. Wagner; in Applied Surface Science (2002), Vol. 197-198, p. 862-867